Available online at www.sciencedirect.com
SCIENCE DIRECT®
Journal of Chromatography A, 1055 (2004) 29–39
JOURNAL OF CHROMATOGRAPHY A
www.elsevier.com/locate/chroma

Model-based optimization of a preparative ion-exchange step for antibody purification

David Karlsson, Niklas Jakobsson, Anders Axelsson, Bernt Nilsson*

Department of Chemical Engineering, Lund University, P.O. Box 124, SE-221 00 Lund, Sweden

Received 3 March 2004; received in revised form 18 August 2004; accepted 20 August 2004

Abstract

A method using a model-based approach to design and optimize an ion-exchange step in a protein purification process is proposed for the separation of IgG from a mixture containing IgG, BSA and myoglobin. The method consists of three steps. In the first step, the model is calibrated against carefully designed experiments. The chromatographic model describes the convective and dispersive flow in the column, the diffusion in the adsorbent particles, and the protein adsorption using Langmuir kinetics with mobile phase modulators (MPM). In the second step, the model is validated against a validation experiment and analyzed. In the third and final step, the operating conditions are optimized. In the optimization step, the loading volume and the elution gradient are optimized with regard to the most important costs: the fixed costs and the feed cost. The optimization is achieved by maximizing the objective functions productivity (i.e. the production rate for a given amount of stationary phase) and product yield (i.e. the fraction of IgG recovered in the product stream). All optimization is conducted under the constraint of 99% purity of the IgG. The model calibration and the analysis show that this purification step is determined mainly by the kinetics, although as large a protein as IgG is used in the study. The two different optima resulting from this study are a productivity of 2.7 g IgG/(s m^3) stationary phase and a yield of 90%. This model-based approach also gives information of the robustness of the chosen operating conditions. It is shown that the bead diameter could only be increased from 15 μm to 35 μm with maximum productivity and a 99% purity constraint due to increased diffusion hindrance in larger beads.

Keywords: Protein purification; Antibody production; Ion-exchange modeling; Model calibration; Optimization

1. Introduction

The development of biotechnological products is becoming more and more expensive [1]. One type of protein attracting a great deal of attention in the biopharmaceutical industry is antibodies [2]. The cost of producing antibodies is, however, high, mainly due to the downstream processing, which constitutes 80% of the total cost [3]. This includes not only the fixed costs and cost of the high-value products but also the costs involved in developing the processes, not least labor cost. Consequently, a cheap method of designing and optimizing a purification step is extremely important.

It is believed that it will be possible to reduce the number of labor-intensive experiments, thereby shortening the time and reducing the cost, by modeling and simulation in the design and optimization of a process. This requires a methodology employing accurate models validated by carefully designed experiments when developing a new separation step in the downstream process. The model employed should preferably be based on an understanding of the underlying physical mechanisms. This type of model will have a predictive capacity even when experiments are lacking, and will also be very useful for parameter studies.

A widely employed preparative antibody purification step in the biotech industry is ion-exchange chromatography [4]. It is commonly used to separate feed streams that consist of a range of components with different interaction behavior. The best pH and buffer conditions for separation are often deter-

* Corresponding author. Tel.: +46 46 222 8088; fax: +46 46 222 4526.
E-mail address: bernt.nilsson@chemeng.lth.se (B. Nilsson).

0021-9673/$ – see front matter © 2004 Elsevier B.V. All rights reserved.
doi:10.1016/j.chroma.2004.08.151

mined from a retention map [5]. Adsorption is carried out at a constant, low salt concentration while elution is performed at a high salt concentration. It is now becoming more common to use a linear salt concentration gradient. Thus, a linear gradient of increasing mobile phase salt is introduced into the elution step. This technique allows the protein to be concentrated during loading, and to be eluted without substantial dilution if a normal gradient is used.

Model-based optimization of chromatographic columns [6–8] is difficult and cannot be achieved solely by analytical solutions of the equations of chromatography. The high concentration that may arise inside the column during loading, results in competitive multi-component binding, which implies that the prediction of adsorption and mass transport behavior requires the use of numerical techniques [9]. Optimizing the operating conditions in ion-exchange chromatography demands descriptions such as steric mass action (SMA) [9] or, as in this study, a Langmuir description with mobile phase modulators (MPM) [10], which can describe both multi-component protein adsorption and salt-induced elution. Other phenomena such as diffusion may also be important in the separation of macromolecules as the diffusion rate is often rate limiting [11].

The approach presented here is suitable in capture, the first purification step after the expression system, and in the intermediate steps following the capture. The optimization method developed in this work requires just a few additional experiments besides those required for the retention map and a validation experiment. The calibrated and validated model can be used to gain greater insight into the optimization of ion-exchange chromatography.

2. Theory — models, simulation techniques and optimization

The model used to describe the purification step may consist of two or three parts. The description of the convective and dispersive flow in the column and the adsorption kinetics are included in both cases. The diffusive transport within the adsorbent particles is included in the latter case [12]. Langmuir kinetics with a mobile phase modulator is used to describe protein adsorption [10]. In this work, the shapes of the elution peak and breakthrough curve are dependent on a dispersion coefficient and the adsorption rate. If the particle description is included the shape is also dependent on a diffusion coefficient and a mass transfer coefficient.

2.1. The column model

The chromatography column is assumed to be filled with beads of equal size. The convective flow is subject to intermixing, defined by an axial dispersion coefficient, D_{ax} (m^2/s). The column model for component i is described by the following equation:

$$\frac{\partial c_i}{\partial t} = D_{ax}\frac{\partial^2 c_i}{\partial x^2} - v_{int}\frac{\partial c_i}{\partial x} - \frac{1-\varepsilon_c}{\varepsilon_c}F \tag{1}$$

If a detailed model of the particle is used, the help variable, F, describes the mass transfer from the mobile phase to the surface of the particle using a film mass transfer coefficient, k_f (m/s) [12]:

$$F = \frac{3}{R}k_{f,i}(c_i - c_{p,i|r=R}) \tag{2}$$

otherwise, an adsorption model of the Langmuir type describes F [13].

$$F = \frac{\partial q_i}{\partial t} \tag{3}$$

Here, ε_c is the void fraction in the packed bed (m^3 mobile phase/m^3 column), x the axial coordinate along the column (m), v_{int} the interstitial velocity (m/s), c_i the concentration of component i in the mobile phase (kmol/m^3), R the radius of the bead (m), $c_{p,i|r=R}$ the concentration of component i at the surface of the bead (kmol/m^3), q_i the concentration of component i in the stationary phase, denoted sp (kmol/m^3 sp), and t is the time (s).

The column equation is subject to two different boundary conditions. A Robin condition describes the column inlet:

$$\frac{\partial c_i}{\partial x} = \frac{v_{int}}{D_{ax}}(c_i - c_{inlet,i}), \quad \text{at } x = 0 \tag{4}$$

where $c_{inlet,i}$ is the inlet feed concentration (kmol/m^3) and c_i is the concentration just inside the column (kmol/m^3), which may be slightly lower than $c_{inlet,i}$ due to dispersion at the inlet. At the outlet where x is equal to L, the length of the column (m), only convective transport is considered and can thus be described by a Neumann condition.

$$\frac{\partial c_i}{\partial x} = 0, \quad \text{at } x = L \tag{5}$$

2.2. The particle model

The mass transfer within the particle to the adsorption sites is a diffusive process described by D_e, the effective diffusion coefficient (m^2/s). The particle is assumed to be spherical with radius R. The particle model for component i is described by the following equation:

$$\frac{\partial c_{p,i}}{\partial t} = \frac{D_{e,i}}{\varepsilon_{p,i}}\left(\frac{\partial^2 c_{p,i}}{\partial r^2} + \frac{2}{r}\frac{\partial c_{p,i}}{\partial r}\right) - \frac{1}{\varepsilon_{p,i}}\frac{\partial q_i}{\partial t} \tag{6}$$

where $c_{p,i}$ is the concentration of component i in the pore liquid (kmol/m^3), r the radius coordinate (m) and $\varepsilon_{p,i}$ is the particle porosity fraction for component i (−), i.e. the volume accessible to component i in the particle divided by the total particle volume. The boundary condition is a Robin condition

at the particle surface, which couples the particle description to the column model, see Eq. (1).

$$\frac{\partial c_{p,i}}{\partial r} = \frac{k_{f,i}}{D_{e,i}}(c_i - c_{p,i|r=R}), \quad \text{at } r = R \tag{7}$$

In the center of the particle the mass flux, and thus its derivative, is zero and is described by a Neumann condition:

$$\frac{\partial c_{p,i}}{\partial r} = 0, \quad \text{at } r = 0 \tag{8}$$

2.3. Adsorption — the Langmuir MPM model

The protein mixture studied contains proteins of various sizes. It is assumed that the binding sites are uniformly distributed and have equi-accessible fixed charges at the adsorptive surface. Langmuir kinetics [12], see Eq. (9), describes the adsorption and desorption of the protein and these are regarded as competitive processes in which the salt concentration affects the retention of the protein. Because salt is considered to be inert, dq_{salt}/dt is zero. During the binding step, $k_{ads,i}$, the adsorption coefficient of component i (m^3/(kmol s)), is much larger than $k_{des,i}$, the desorption coefficient of component i (s^{-1}), while at elution $k_{des,i}$ dominates.

$$\frac{\partial q_i}{\partial t} = k_{ads,i} c_{x,i} q_{max,i} \left(1 - \sum_{j=1}^{N} \frac{q_j}{q_{max,j}}\right) - k_{des,i} q_i \tag{9}$$

Here, $q_{max,i}$ and $q_{max,j}$ are the maximum concentrations of components i and j in the stationary phase (kmol/m^3 sp); q_i and q_j are the concentrations of components i and j in the stationary phase (kmol/m^3 sp), and N is the number of interacting components. If the particle description is included in the model, $c_{x,i}$ is the concentration in pore liquid (kmol/m^3), otherwise it is the bulk concentration (kmol/m^3).

The model can be used for the loading step as well as the elution step by using mobile phase modulators [10], defined by Eqs. (10) and (11):

$$k_{ads,i} = k_{ads0,i} e^{\gamma_i S} \tag{10}$$

$$k_{des,i} = k_{des0,i} S^{\beta_i} \tag{11}$$

where S is the concentration of the elution component, often salt, and $k_{ads0,i}$ (m^3/(kmol s)) and $k_{des0,i}$ (m^3/(kmol s)) are constants. β_i (−) is a constant describing the ion-exchange characteristics and γ_i (m^3/kmol) describes the hydrophobicity [10]. Under loading conditions, S is given by the buffer salt concentration and salt from the proteins, i.e. $k_{ads,i} \approx k_{ads0,i}$ and $k_{des,i} \approx 0$ unlike, the elution conditions ($S > 0$) where $k_{ads,i}$ is reduced by the factor $e^{\gamma S}$ ($\gamma < 0$) and $k_{des,i}$ is increased by the factor $S^{\beta i}$. In this study, it was assumed that there are no hydrophobic interactions, which means that γ_i is equal to zero. Although hydrophobic interactions are neglected their effect can be seen from a parameter study of the model by tuning the factor, γ_i.

2.4. Simulation techniques

The simulations were performed in MATLAB [14] using BioSepToolbox [15,16]. Each partial differential equation in the model is discretized in space to give a set of ordinary differential equations using the method of lines (MOL). The space is divided into a set of grid points, where each grid point contains a discretized ordinary differential equation. A three-point, finite-difference method was used to discretize the column and the particles. For the case including particle description the number of grid points was set to 50 in the column and 5 in the particle. Otherwise 60 grid points were used in the column, which is sufficient to avoid numerical dispersion. The discretized model was solved with a standard solver for ordinary differential equations (ODE15S) in MATLAB.

2.5. Chromatographic optimization

To optimize a non-linear preparative chromatographic ion-exchange step four types, of objects have to be considered: objective functions, design parameters, decision variables, and constraints [6,17,18]. These are presented are described below.

2.5.1. Objective functions

For successful optimization, it is important to choose a suitable objective function to minimize or maximize. In this study three different objective functions were used. One of the most common objective functions for preparative chromatography is the productivity, PR_i (kg/(s m^3 sp)), of a component i, which gives the production rate for a given amount of stationary phase:

$$PR_i = \frac{c_{i,Load} V_{Load} Y_i}{t_c V_{sp}} \tag{12}$$

where $c_{i,Load}$ is the feed concentration (kg/m^3) of component i in the loading step, V_{Load} is the loading volume (m^3), Y_i is the yield of component i, t_c is the cycle time (s), and V_{sp} is the volume of stationary phase used in the column (m^3). Maximizing the productivity will give a measure of the highest possible amount of protein that can be purified per unit time per unit stationary phase. The yield is calculated as the ratio between the amount of component i in the elution fraction with the required purity divided by the amount of component i loaded, see Eq. (13):

$$Y_i = \frac{\int_{t_1}^{t_2} c_i \, dt}{c_{i,Load} t_{Load}} \tag{13}$$

where t_1 and t_2 are the cut times (s) and t_{Load} is the loading time (s). The yield is one of the most important objective functions if the product is very expensive, which is often the case with biopharmaceuticals.

Combining the objective function for productivity and yield gives the normalized earning (NE) objective function,

Table 1
The objective functions used in the normalized earning objective function depending on which cost is dominant

Dominant cost	w	Maximize
Fixed costs	1	Productivity
Feed cost, i.e. the value of the product lost	0	Yield

i.e. the relation between fixed costs, FiC, and feed cost, FeC [19], which, in some sense, is how much can be produced and is expressed as kg per euro. The fixed costs include the cost of the system, the adsorbent packing, the labor, etc. and the feed cost is simply the cost per unit feed, i.e. the value of the product lost. Costs not included in this study are the solvent cost, which is the cost of solvents used in the downstream process, and the energy used in the process. These costs are often not of importance when dealing with the purification of antibodies. Two extreme cases can be envisioned, see Table 1 using the ratio w, see Eq. (14), and the objective function, see Eq. (15), depending on which cost is dominating

$$w = \frac{\text{FiC}}{\text{FiC} + \text{FeC}} \tag{14}$$

$$\text{NE}_i = w\frac{\text{PR}_i}{max(\text{PR}_i)} + (1-w)\frac{Y_i}{max(Y_i)} \tag{15}$$

2.5.2. Design parameters

The most typical parameter in a preparative chromatographic purification step is the concentration of the feed constituents. Other parameters in this study are buffer, eluting salt, stationary phase material and the pH at which the separation is carried out. Parameters cannot be changed during the optimization process. They are pre-scouted or determined by the composition of the fermentation broth.

2.5.3. Decision variables

A chromatographic purification step consists of many decision variables, which leads to a high degree of freedom. The values of these variables are changed to maximize or minimize the objective function to obtain an optimal purification step. Typical decision variables are loading, washing and elution times, salt concentration, the flow rate in the different steps, column length, column diameter, and the gradient in the elution step. To limit the degree of freedom the effects of two variables were studied: the loading time and the gradient in the elution. These variables control the cycle time and the amount of protein purified. All other decision variables were constant during the study and were therefore treated as parameters.

2.5.4. Constraints

The optimization process can only be carried out in an operating window defined by the constraints. These can be defined as either physical or quality constraints. Physical constraints include solubility and activity while examples of quality constraints are yield and purity [20]. In this study, the purity was set to 99%, and the yield was treated as an objective function. The solubility and activity were assumed to be within a suitable range.

3. Working procedure

The procedure used in this work to optimize a chromatographic ion-exchange column is divided into three steps, see Fig. 1. The first step deals with model calibration [13]. The calibrated model is validated against an experiment and analyzed in step 2. In the last step optimization is performed with the validated and calibrated model.

3.1. Model calibration

3.1.1. Shape parameters

The effective diffusion coefficient, the film mass transfer coefficient, and the accessible particle porosity can be considered as shape parameters as they are to same degree dependent on the bead and column shape. To determine these parameters column breakthrough experiments are performed [21]. These are single component experiments and are carried out under non-binding conditions with four different flows. The parameters are calibrated using a non-linear least-squares regression method in MATLAB. The shape parameters are calibrated at the same time for the flow used. The effective diffusion coefficient and the particle porosity are considered

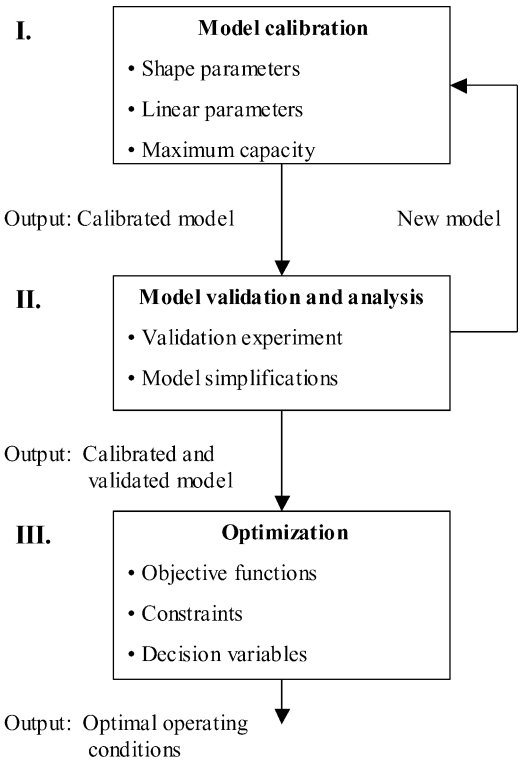

Fig. 1. The procedure employed in model-based optimization of an ion-exchange step. The procedure is divided into model calibration, model validation and analysis, and finally optimization.

to be independent of the flow rate, which is not the case for the film mass transfer coefficient. The dispersion coefficient was determined using an empirical correlation where the Peclet number was set to 0.5 [22]:

$$Pe = \frac{v_{int} d_p}{D_{ax}} \quad (16)$$

where d_p is the bead diameter (m).

3.1.2. Linear parameters

To calibrate $k_{des0,i}$, $k_{ads0,i}$, and β_i, gradient elution experiments with different gradients are performed. The parameters are tuned in order to fit the simulated retention times for the different proteins to the experimental ones. This is done manually by changing β_i and $k_{ads0,i}/k_{des0,i}$ in an iterative process, using different elution gradients [13].

3.1.3. Maximum capacity

The maximum adsorbent capacity is determined by frontal chromatography with pure components with concentrations on the non-linear part of the adsorption isotherm. The value of the maximum capacity, $q_{max,i}$, in the model is tuned to match the experimental breakthrough volume. The value of $q_{max,i}$ determines the equilibrium for the different proteins and should be approximately constant for the same breakpoint, regardless of the concentrations of salt and protein, if concentrations on the linear part of the adsorptions isotherm are used to estimate the linear parameters. Using the calibrated value of $q_{max,i}$ in the elution gradient experiment can be used to check this. If this is not the case, an iterative calculation procedure between the capacity and the linear parameters is necessary until the correct value of $q_{max,i}$ is obtained.

3.2. Model validation and analysis

To ascertain that the model is correct, a validation experiment is performed for a protein mixture with salt content and protein concentrations not used in the model calibration. If the model proves satisfactory after the validation, analysis of the parameters in the model is performed. The analysis is partly the result from the model calibration and partly from sensitivity calculations performed after the validation. After this analysis the model is simplified, if possible, in order to reduce the number of parameters in the model and to speed up the calculations.

3.3. Optimization

First the decision variables are chosen; in this study the loading time and the elution gradient. The other decision variables were considered to be design parameters. The optimization is performed as a parameter study of the decision variables. Following this, the constraint is applied, in this study the purity. This is done using the fractionizer in BioSepToolbox [16,23] where the volume fraction of the product is calculated according to the purity constraints. Finally, the objective function is calculated at each point in the parameter study to give the optimal operating conditions.

4. Materials and methods

4.1. Materials

The column used in the chromatography experiments were pre-packed columns (diameter 6.4 mm, length 30 mm) filled with a strong anion-exchanger, RESOURCE 15 Q, 1 ml (no. 920408) supplied by Amersham Biosciences (Uppsala, Sweden). The beads have a diameter of 15 μm. The column used to analyze the fractions was a gel filtration column, TSK-G 3000 SWXL (diameter 7.8 mm, length 30 cm) from Toso-Haas (Tokyo, Japan). In this column the bead diameter was 5 μm.

Three different components were used in the experiments: bovine serum albumin (BSA) (A-1900, Lot no. 75H9305), and myoglobin (M-4132, Lot no. 048H7017), both obtained from Sigma (Steinheim, Germany) and polyclonal IgG kindly provided from Biovitrum AB, Stockholm, Sweden. The IgG protein solution consists of four different clonals and has a concentration of 15.7% (w/w). Trizma base (T-1503, Lot no. 120K5403), was also obtained from Sigma. NaCl was obtained from Merck (Darmstadt, Germany).

The chromatography experiments were carried out on an ÄKTA purifier 100 system from Amersham Bioscience.

4.2. Methods

Optimal pH was scouted to 8.7, which was proven to give good separation between IgG, BSA, and myoglobin.

4.2.1. Breakthrough experiments — determination of shape parameters D_e, ε_p and k_f

To obtain valid shape parameters single component breakthrough experiments were carried out at four different flow rates: 1, 2, 3, and 4 ml/min. The concentration of the proteins was 0.5 mg/ml in all experiments. A 20 mM Tris buffer with 1 M NaCl at a pH of 8.7 was used. The high salt concentration was used to prevent protein binding to the stationary phase.

4.2.2. Gradient experiments to determine the linear parameters in the model

The values of $k_{ads0,i}$, $k_{des0,i}$ and β_i in the Langmuir MPM model can be found by running gradient elution experiments with different gradients [24]. The linear gradients used for parameter estimation were 20, 25, 30, 35, 40, 50, and 60 column volumes (CV). The inlet concentrations were 0.20 mg/ml IgG, 0.19 mg/ml BSA and 0.12 mg/ml myoglobin. The buffer was a 20 mM Tris buffer at a pH of 8.7 and the elution buffer was 20 mM Tris buffer, pH 8.7, with 1 M NaCl. The flow rate for all gradient elution experiments was 1 ml/min. The conductivity in the loading step was about 0.82 mS/cm and at the end of the elution about 82 mS/cm. The loading step lasted

Table 2
Protein concentration and the total salt concentration during the breakthrough experiments to determine the maximum capacity for each protein

Protein	Protein concentration (mg/ml)	Salt concentration (kmol/m^3)
IgG	6, 8, and 10	0.012, 0.016, and 0.015
BSA	8 and 10	0.03 and 0.034
Myoglobin	1, 2, and 3	0.0085, 0.011, and 0.0079

2 CV and the column was washed with 8.5 CV of buffer. The experimental results were compensated for dead volumes in the system to isolate the behavior due to the column.

4.2.3. Experiments to determine the maximum capacity, q_{max}

In this study, the capacity breakthrough experiments had to be performed at sufficiently high protein concentration to lie in the non-linear part of the isotherm. Experiments were performed at conditions listed in Table 2.

The flow rate was 1 ml/min and the buffer was 20 mM Tris buffer, pH 8.7, supplemented with NaCl to obtain the salt concentration in Table 2.

4.2.4. Experiments to determine the dead volume in the chromatography system

The ÄKTA Purifier system has a relatively low dead volume for the sample when using a 2 ml loop or a superloop in the injection of the sample. The dead volume in the ÄKTA Purifier system was found to be 0.14 ml in the experimental set-up used.

4.2.5. Validation experiment

To validate the model a validation experiment was performed with conditions that differed from those in the model calibration. A mixture of 3 mg/ml IgG, 0.5 mg/ml BSA, and 1 mg/ml myoglobin was loaded onto a column using a superloop. The experiment was performed at a flow rate of 1.2 ml/min. The buffer was a 20 mM Tris buffer at a pH of 8.7, and the elution buffer was 20 mM Tris buffer, pH 8.7, with 1 M NaCl. The loading was 9.2 CV, the washing 5 CV and the elution gradient 32 CV. The conductivity in the loading step was 1.22 mS/cm and in the elution step 82 mS/cm. Fractions were collected during the entire experiment and were analyzed by gel filtration to determine the presence of the different components.

5. Results and discussion

5.1. Model calibration

The model that was calibrated against the column experiments includes the particle description. The ReSource ion-exchanger column contains monosized particles with very large pores. The large pores make it difficult to measure the column void with, for example, latex particles. Therefore, the column void was not measured experimentally, but was set to 0.32 in the model based on previous experience [13]. The void fraction is relatively low, but this value is considered reasonable as the column was industrially packed. Physical data for the proteins used in this study are presented in Table 3.

Table 3
Physical data for proteins used in this study

Protein	Molecular weight (kDa)	pI	Stoke radius (nm)
IgG	150[b]	5–8.5[b]	5.6[a]
BSA	67[e]	4.9[c]	3.6[a]
Myoglobin	18[d]	7–8[d]	1.9[a]

[a] [27].
[b] [30].
[c] [31].
[d] [32].
[e] [33].

Table 4
Particle porosity, diffusion coefficient and film mass transfer estimated from single component breakthrough experiments

Protein	ε_p	D_e (m^2/s)	k_f (m/s)
IgG	0.50	3.5×10^{-12}	1.1×10^{-4}
BSA	0.59	5.4×10^{-12}	1.6×10^{-3}
Myoglobin	0.66	7.0×10^{-12}	3.2×10^{-2}

5.1.1. Shape parameters

The shape parameters were estimated from the single component breakthrough experiments, see Table 4. The estimated value for each parameter is the average value obtained at four different flow rates.

An example of parameter estimation is shown in Fig. 2. The estimation shows that it is difficult to find the film mass transfer coefficient at which the sum of the squares is almost the same for all coefficients over 10^{-5}. One explanation may be that the film mass transfer coefficient is probably not rate limiting, and is difficult to see in the experiment. The effective diffusion coefficients estimated for the different proteins in this study are 10 times lower than those obtained by holo-

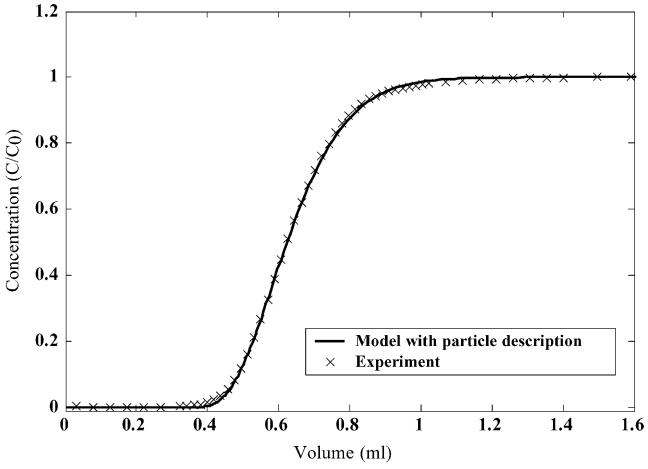

Fig. 2. The model fitted to results from an IgG breakthrough experiment by changing the diffusion coefficient, the particle porosity and the film mass transfer coefficient at a flow rate of 3 ml/min.

Table 5
Diffusion data from different sources

Protein	ε_p	D_e (m^2/s)	Method
IgG	0.51	1.5×10^{-11}	ESPI[a]
	0.46	2.6×10^{-12}	Chromatography[b]
BSA	0.44	2.1×10^{-11}	ESPI[a]
	0.55	5.9×10^{-12}	Chromatography[b]
Lysozyme	0.65	7.3×10^{-11}	ESPI[a]
Myoglobin	0.73	2.5×10^{-11}	Chromatography[b]

[a] [26].
[b] [27].

graphic methods [25]. Data from electronic speckle pattern interferometry (ESPI) measurements also show higher values for the effective diffusion coefficients but almost the same particle porosity [26], see Table 5.

The ESPI study includes the same proteins as in this study except for the smallest one, where lysozyme was used instead of myoglobin. The values of D_e in the present chromatography breakthrough experiments are probably lower due to the cross-linked Source gel used in this study instead of the non-cross-linked agarose in the ESPI study. According to the Stokes–Einstein equation myoglobin can be assumed to have almost the same diffusion coefficient as lysozyme. Data from other studies using chromatographic breakthrough experiments show parameter values in roughly the same range as in this study, even when an agarose gel was used [27].

5.1.2. Linear parameters

Gradient elution experiments were performed and the retention times for the three components were corrected for the dead volume in the experimental equipment. The ratio k_{ads0}/k_{des0} and the parameter β in the Langmuir MPM model were adjusted to find the correct peak position at different elution gradients at pH 8.7. The various parameters determined for the three proteins for the Langmuir MPM model are reasonable [13] and can be found in Table 6.

The estimated parameters for the elution step with a salt gradient of 30 CV are compared with the experimental results in Fig. 3. The peak position is estimated from first-moment calculations of the absorbance [28], not the maximal absorbance at the ÄKTA. As can be seen from the chromatograms, the peak positions are estimated with good accuracy for the model at a gradient of 30 CV. The peaks are, however, a little wider and not as high as in the experiment. This is due to the shape parameters calibrated from the breakthrough experiments, which limit the influence of the kinetic parameters on the peaks at values of k_{des0} over 50. Another

Table 6
The estimated linear parameters in the Langmuir MPM model

Protein	k_{des0}/k_{ads0}	k_{des0} (kmol/(m^3 s))	β
IgG	1.3×10^{-3}	50	1.12
BSA	1.7×10^{-2}	50	3.2
Myoglobin	6.0×10^{-4}	50	0.61

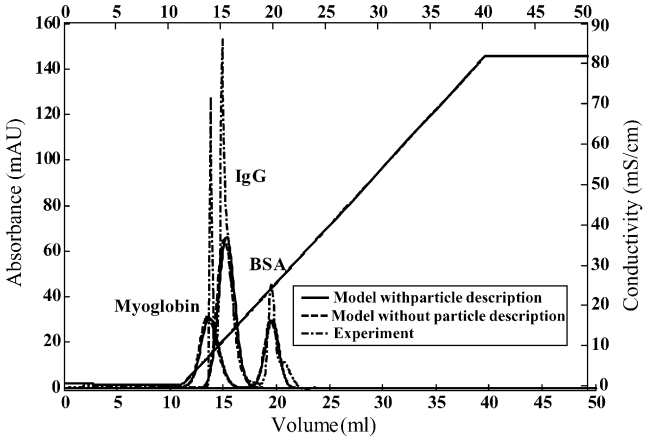

Fig. 3. Comparison between a case including particle description and one without particle description, and the experiment with an elution gradient of 30 CV.

explanation may be that UV-absorbance calculated from calibration curves for each component not gives the same combined result as the total UV-absorbance in the experiment. The small peak after the BSA peak contains one of the IgG clonals and was not used to evaluate the procedure.

The mean error in the peak position at seven gradients (20, 25, 30, 35, 40, 50, and 60 CV) used for parameter estimation is ±2.8% for IgG, ±0.8% for BSA and ±3.0% for myoglobin. The lower accuracy for IgG and myoglobin is probably due to the fact that they have a small mean charge, which makes them more sensitive to salt dynamics, which is not taken into account in the model.

5.1.3. Maximum capacity

The maximum capacity, q_{max}, was determined by breakthrough chromatography experiments with pure components at high concentration. The capacities were 5.40×10^{-4} kmol/m^3 sp for IgG, 1.04×10^{-3} kmol/m^3 sp for BSA

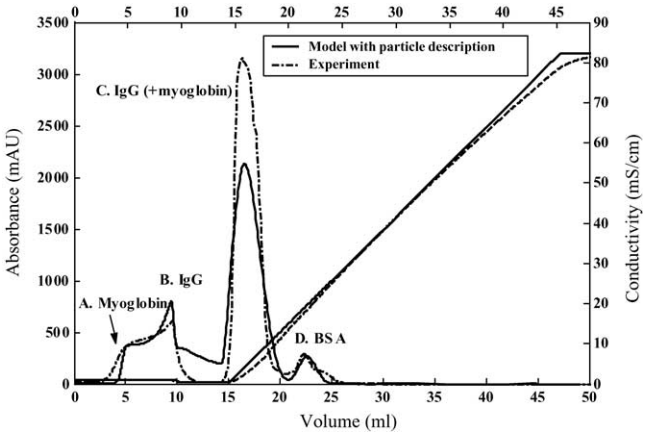

Fig. 4. The validation experiment with an elution gradient of 32 CV compared to the case including the particle description. The first breakthrough (A) is myoglobin and the second (B) is IgG. The first elution peak consists (C) almost only of IgG with a small fraction of myoglobin. The last peak (D) is BSA.

Table 7
Operating conditions at maximum objective function value for different objective functions

Objective function	Cost	Max objective function value	Loading volume (ml)	Elution gradient (ml and CV)	Cycle time (min)	Elution volume (ml)	Fraction volume (ml)
Productivity	Fixed	2.7 g/(s m^3 sp)	23	91 and 94	39	13	8
Yield	Feed	90%	8	240 and 249	34	21	11

and 0.75×10^{-3} kmol/m^3 sp for myoglobin. An iterative calculation process between the elution gradient experiment and the capacity experiment were necessary to determine the capacities for IgG and myoglobin [29].

5.2. Validation and analysis

The validation experiment was performed as a gradient elution experiment with protein concentrations that were not used in the parameter estimation. The salt concentration in the loading step was also different from that used in the parameter estimation. Although much higher concentrations of the proteins were used than in the model calibration, the model fitted the validation experiment with relatively good accuracy, see Fig. 4. The first breakthrough is myoglobin and the second is IgG. In the washing step the UV-absorbance for the experiment approaches zero. This is not accounted for in the model and some of the IgG and myoglobin was washed out, causing a loss in peak height in the elution step. In the elution step, the peaks in the model are at the same positions as in the validation experiment. The last peak is BSA and has almost the same shape in the simulation as in the experiment. The first peak is almost only IgG, which both the experiment and model shows. Most of the myoglobin is displaced in the loading and washing step.

An analysis of the model shows that the peak positions are mainly determined by the linear parameters. Although such a large protein as IgG is used, the effective diffusion and film mass transfer are of less importance. Only narrow peaks in the elution will be influenced. Another observation from the model calibration was long computation times. One calculation could take 1–2 h, which would make the computation time for the optimization rather long, 4–5 days. Based on this, the model was simplified. The simplified model did not include the particle description, but still showed almost the same behavior if only the dispersion coefficient was changed, see Fig. 3. The computation time for this model was about 1–2 min. This model was used in the optimization.

5.3. Optimization

The optimization was carried out as a parameter study by changing the decision variables, i.e. the loading volume and the elution gradient. The gradient is defined as the number of column volumes required to obtain the maximum salt concentration, in this study 1 M. The elution is stopped when the IgG peak concentration has fallen to 0.5% of the feed concentration. The batch cycle ends with the regeneration step. This is one of the major benefits of model-based optimization compared to experimental-based optimization, because it is possible to perform calculations for each component. During the optimization the inlet protein concentrations were set to 0.4 mg/ml IgG, 0.4 mg/ml BSA and 0.2 mg/ml myoglobin. The salt concentration was 0.009 M during the loading step, and the washing and regeneration volumes were fixed at 6 ml (6 CV). Using the normalized earning objective function the combined optimum for productivity and yield was studied by tuning w from 0 to 1, see Table 1. The purity constraint was set to 99%.

5.3.1. Productivity

The operating conditions for maximal productivity are given in Table 7. As can be seen in Fig. 5, the chromatogram has a rather wide breakthrough for myoglobin in the loading step and, the IgG breakthrough stops just after it has started to recover as much as possible of IgG in the elution step. The BSA peak is very narrow because of the salt step in the regeneration step and has a peak concentration of about 60 mg/ml.

To ensure robust operating conditions in the ion-exchange step it is important to be sure that the loading volume and the elution gradient volume are not in a region with steep edges, see Fig. 5. A small deviation from the optimal operating point can have a considerable impact on process performance if the operating conditions are close to the steep edges. The optimal operating conditions in the case seen in Fig. 5 is in a relatively flat region, indicating that the purification step is robust at maximal productivity for the decision variables studied.

5.3.2. Yield

When the yield is the dominating factor a flat gradient is often obtained, see results in Table 7 and Fig. 6. The narrow BSA peak has a peak concentration of only 15 mg/ml due to the short loading time.

If the highest priority is given to maximum yield, the optimum will give a very flat elution gradient, which can clearly be seen in the optimization plot in Fig. 6. The yield decreases again at very small loading volumes because the small product peak will have a larger part included in the impurities. The optimum will also lie on the edge of the elution gradient volume in the parameter study. As the optimum has a very shallow elution gradient a small salt step could probably also be used in this case. These operating conditions are also robust as there is no steep edge near the maximum yield point.

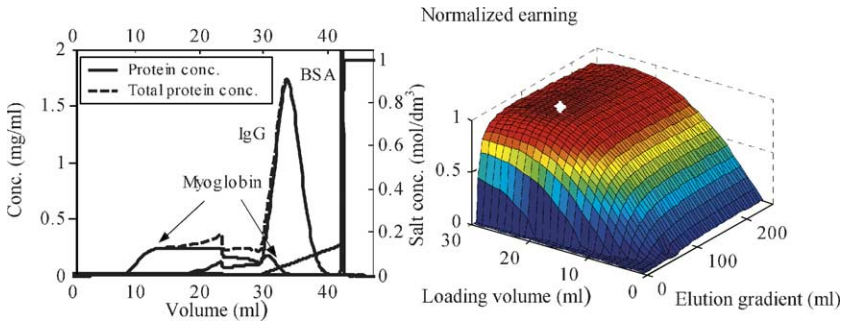

Fig. 5. The chromatogram at maximum productivity and the optimization plot with 99% purity and productivity as the most important objective function. Maximum productivity is indicated out as an asterisk (*).

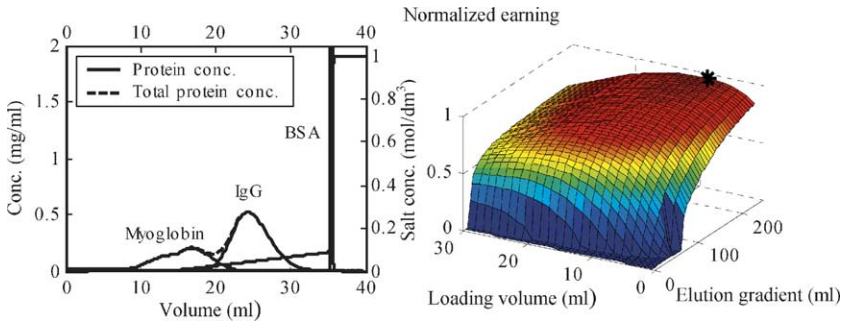

Fig. 6. The chromatogram at maximum yield and the optimization plot with 99% purity and yield as the most important objective function. Maximum yield is indicated by as an asterisk (*).

5.3.3. *Productivity and yield*

If the normalized earning objective function Eq. (13) is maximized different optimum will be obtained depending on the relative costs. The operating conditions will vary according to Fig. 7. The two special cases of productivity and yield as the dominating factor are shown as endpoints of the curve. These cases are also given in Table 7. A horizontal line at an elution volume of approximately 21 ml near maximum yield is obtained. The elution volume would probably be larger if the parameter study contained a larger range of elution gradients. The optimal operating conditions vary considerably depending on the object function. The loading volume increases three times from maximal yield to maximal productivity, while the elution volume decreases by almost 50%.

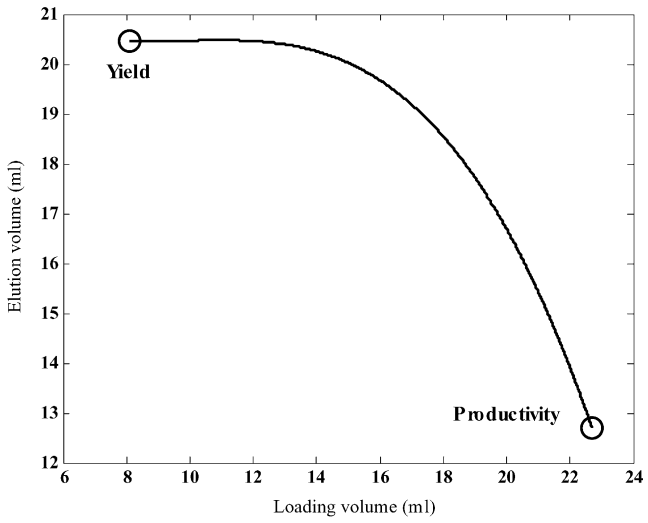

Fig. 7. Optimal operating conditions depending on the most important cost, i.e. productivity or yield.

5.3.4. *Analysis of the influence of diffusion*

One way to decrease costs when scaling up a purification step is to choose a cheaper stationary phase than the Source gel. This can easily be studied using the present model-based approach by investigating the effect on diffusion of increasing the bead diameter in the model including the particle description, at maximum productivity and 99% purity, see Fig. 8. The fraction volume is defined as the volume of product obtained in the elution step.

It is only possible to increase the bead diameter to 35 μm, which will make it difficult to use a stationary phase based on agarose gel under these conditions and parameters. Agarose beads often have a larger diameter than the Source beads. If myoglobin is considered to be inert in this step, i.e. a separation between only IgG and BSA and separated in next purification step, it is possible to use a larger bead diameter and this step will probably be performed as negative chromatography. Reducing the requirement on the purity, on the other hand, gives the same pattern as with 99% purity, but the op-

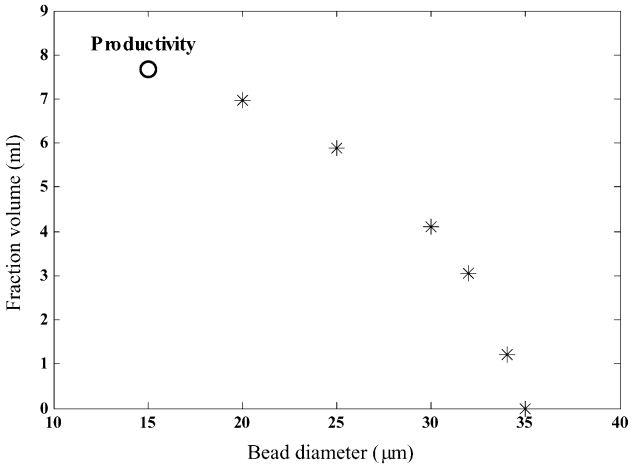

Fig. 8. The fraction volume at different bead diameters at maximum productivity and 99% purity.

timum is moved closer to the steep edges in the optimization plot.

6. Conclusions

The model-based optimization method suggested in this work includes model calibration, model validation and analysis, and optimization. It has been proven to be an efficient approach in process development. Apart from the normal experimental work some additional experiments have to be performed to obtain the parameters used in the model. This optimization method gives good predictability. Model-based optimization results in less experimental work in process design as a whole compared with optimization based on experiments. This will lead to less labor-intensive design, which will save time and money.

Based on experience gained with the present protein model system myoglobin appears to be very sensitive to the salt concentration at pH 8.7, which the model has problems to describing at steep elution gradients, as also reported in experimental work by Ebershold and Zydney [29]. The model calibration and analysis shows that this purification step is mainly determined by the kinetics despite the fact that as large a protein as IgG was used in the study. Changing the diffusion coefficient 10 times did not affect the linear parameters. This is probably due to the small Source beads (15 μm) used.

An advantage of the model-based approach is that optimal operating conditions can easily be calculated depending on the objective function chosen. Besides the quantification of the optimal conditions, in this case a productivity of 2.7 g/(s m^3 sp) and a yield of 90%, additional information is obtained from the optimization plots. The robustness of the operating conditions can easily be seen for the decision variables studied.

The optimum given on a small scale also provides a platform for modeling of scale-up and optimization of protein purification processes on production scale. Furthermore, the mechanistic structure of the model makes it easy and informative to perform parameter studies for the separation system being studied.

7. Nomenclature

c_i	concentration of compound i in the mobile phase (kmol/m^3)
$c_{i,\mathrm{Load}}$	mass concentration of compound i in the loading step (kmol/m^3)
$c_{\mathrm{inlet},i}$	inlet concentration of compound i in the mobile phase (kmol/m^3)
$c_{\mathrm{p},i}$	concentration of compound i in the pore liquid (kmol/m^3)
$c_{\mathrm{p},i\|r=R}$	concentration of compound i at the surface of the bead (kmol/m^3)
c_{s}	concentration of salt in mobile phase (kmol/m^3)
$c_{x,i}$	concentration of compound i in the pore liquid or the bulk phase (kmol/m^3)
d_{p}	bead diameter (m)
D_{ax}	dispersion coefficient (m^2/s)
D_{e}	effective diffusion coefficient (m^2/s)
F	help variable
FeC	feed cost (€)
FiC	fixed costs (€)
$k_{\mathrm{ads},i}$	adsorption coefficient, Langmuir MPM (m^3/(kmol s))
$k_{\mathrm{ads0},i}$, $k_{\mathrm{des0},i}$	modulator constants (m^3/(kmol s))
$k_{\mathrm{des},i}$	desorption coefficient, Langmuir MPM (s^{-1})
k_{f}	film mass transfer coefficient (m/s)
L	length of the column (m)
NE_i	normalized earning
Pe	Peclet number
pI	isoelectric point
PR_i	productivity of compound i (kg/(s m^3 sp))
$q_{\mathrm{max},i}$, $q_{\mathrm{max},j}$	maximum concentration in the stationary phase for compound i and j (mol/m^3 sp)
q_i, q_j	concentration in the stationary phase for compound i and j (mol/m^3 sp)
r	radius dimension (r)
R	bead radius (m)
S	concentration of the elution component (mol/m^3)
t	time (s)
t_1, t_2	cut times at given purity (s)
t_{c}	cycle time (s)
t_{Load}	loading time (s)
v_{int}	interstitial velocity (m/s)
V_{Load}	loading volume (m^3)
V_{sp}	stationary phase volume (m^3)
V_{c}	total amount of solution during a cycle (m^3)
w	objective function ratio

x axial coordinate along the column (m)
Y_i yield of comp i

Greek letters
β_i constant describing the ion-exchange characteristic
ε_c void fraction in the column (m^3 mobile phase/m^3 column)
ε_p particle porosity fraction of comp i (m^3 accessible bead/m^3 bead)
γ_i constant describing the hydrophobicity characteristic (m^3/mol)

Acknowledgements

The Swedish Centre for BioSeparation is gratefully acknowledged for financial support. BioInvent International AB, Lund, Sweden and Biovitrum AB, Stockholm, Sweden are also acknowledged for providing materials.

References

[1] H.I. Miller, Nat. Rev. Drug Discovery 1 (2002) 1007.
[2] G. Walsh, Eur. J. Pharm. Biopharm. 55 (2003) 3.
[3] B. Hunt, C. Goddard, A.P.J. Middelberg, B.K. O'Neill, Biochem. Eng. J. 9 (2001) 135.
[4] R.K. Scopes, Protein Purification—Principles and Practice, Springer-Verlag, 1994. Chapter 6.
[5] Amersham Pharmacia Biotech, Ion-Exchange Chromatography—Principles and Methods, Amersham Pharmacia Biotech, Björkgatan 30, SE-75184 Uppsala, Sweden, 1999.
[6] A.M. Katti, P.T. Jageland, Analysis 26 (1998) M38.
[7] A. Felinger, G. Guiochon, J. Chromatogr. A 752 (1996) 31.
[8] A. Jungbauer, O. Kaltenbrunner, Biotechnol. Bioeng. 52 (1996) 223.
[9] C.A. Brooks, S.M. Cramer, Am. Inst. Chem. Eng. J. 38 (1992) 1969.
[10] W.R. Melander, S. El Rassi, C. Horváth, J. Chromatogr. 469 (1989) 3.
[11] P. Roger, C. Mattisson, A. Axelsson, G. Zacchi, Biotechnol. Bioeng. 69 (2000) 654.
[12] F. Carlsson, Mathematical Modelling and Simulation of Fixed-Bed Chromatographic Processes, Lic. Thesis, Dept. of Chem. Eng., Lund University, Lund, Sweden, 1994.
[13] D. Karlsson, N. Jakobsson, K.-J. Brink, A. Axelsson, B. Nilsson, J. Chromatogr. A 1033 (2004) 71.
[14] The MathWorks Inc., MATLAB—The Language of Technical Computing, The MathWorks Inc., 3 Apple Hill Drive, Natick, MA 01760-2098 USA, 2000.
[15] B. Nilsson, A.-K. Nordin, P. Persson, in: M.-N. Pons, J. van Impe (Eds.), Proceedings of Computer Applications in Biotechnology, Elsevier, 2004.
[16] B. Nilsson, Tools for model-based protein separation engineering, in: Proceedings of the 14th European Symposium fo Computer Aided Process Engineering, ESCAPE 14, Lisbon, Portugal, May 17–19, 2004.
[17] S.R. Gallant, S. Vunnum, S.M. Cramer, J. Chromatogr. A 725 (1996) 295.
[18] A. Felinger, G. Guiochon, J. Chromatogr. A 796 (1998) 59.
[19] G. Guiochon, S. Golshan-Shirazi, A.M. Katti, Fundamentals of Preparative and Nonlinear Chromatography, Academic Press, London, 1994.
[20] V. Natarajan, W. Bequette, S.M. Cramer, J. Chromatogr. A 876 (2000) 51.
[21] P. Persson, H. Kempe, G. Zacchi, B. Nilsson, Chem. Eng. Res. Des. 82 (A2) (2004) 1.
[22] T.K. Sherwood, R.L. Pigford, C.R. Wilke, Mass Transfer, McGraw-Hill, 1975.
[23] H. Olsson, M.Sc. Thesis, Dept. of Chem. Eng., Lund University, Lund, Sweden, 2003.
[24] E.S. Parente, B. Wetlaufer, J. Chromatogr. 355 (1986) 29.
[25] C. Mattisson, Ph.D. Thesis, Dept. of Chem. Eng., Lund University, Lund, Sweden, 1999.
[26] D. Karlsson, G. Zacchi, A. Axelsson, Biotechnol. Prog. 18 (2002) 1423.
[27] P.M. Boyer, J.T. Hsu, Am. Inst. Chem. Eng. J. 38 (1992) 259.
[28] O. Levenspiel, The Chemical Reactor Omnibook, OSU Book Stores Inc, Corvallis, OR, 97339, 1996, Chapters 61–68, p. 61.1.
[29] M.F. Ebershold, A.L. Zydney, Biotechnol. Prog. (2004), in press.
[30] Amersham Biosciences, Antibody Purification—Handbook, Amersham Biosciences AB, Björkgatan 30, SE-75184 Uppsala, Sweden, 2002.
[31] C. Fargues, M. Bailly, G. Grevillot, Adsorption 4 (1998) 5.
[32] A. Staby, I. Holm Jensen, I. Mollerup, J. Chromatogr. A 897 (2000) 99.
[33] H. Graf, J.-N. Rabaud, J.-M. Egly, J. Immunol. Methods 139 (1991) 135.